



HAL
open science

Precise morphology control of in-plane silicon nanowires via a simple plasma pre-treatment

Zhaoguo Xue, Wanghua Chen, Xianhong Meng, Jun Xu, Yi Shi, Kunji Chen,
Linwei Yu, Pere Roca i Cabarrocas

► **To cite this version:**

Zhaoguo Xue, Wanghua Chen, Xianhong Meng, Jun Xu, Yi Shi, et al.. Precise morphology control of in-plane silicon nanowires via a simple plasma pre-treatment. *Applied Surface Science*, 2022, 593, pp.153435. <10.1016/j.apsusc.2022.153435>. <hal-04310630>

HAL Id: hal-04310630

<https://polytechnique.hal.science/hal-04310630v1>

Submitted on 22 Jul 2024

HAL is a multi-disciplinary open access archive for the deposit and dissemination of scientific research documents, whether they are published or not. The documents may come from teaching and research institutions in France or abroad, or from public or private research centers.

L'archive ouverte pluridisciplinaire **HAL**, est destinée au dépôt et à la diffusion de documents scientifiques de niveau recherche, publiés ou non, émanant des établissements d'enseignement et de recherche français ou étrangers, des laboratoires publics ou privés.



Distributed under a Creative Commons CC BY-NC 4.0 - Attribution - Non-commercial use - International License

Precise morphology control of in-plane silicon nanowires via a simple plasma pre-treatment

Zhaoguo Xue^{*a, b, c}, Wanghua Chen^{b, d}, Xianhong Meng^a, Jun Xu^b, Yi Shi^b, Kunji Chen^b, Linwei Yu^{*b, c}, Pere Roca i Cabarrocas^{*b}

a. Institute of Solid Mechanics, Beihang University (BUAA), Beijing 100191, China.

b. Laboratoire de Physique des Interfaces et des Couches Minces, CNRS, École Polytechnique, Institut Polytechnique de Paris, 91128 Palaiseau, France

c. National Laboratory of Solid State Microstructures/School of Electronics Science and Engineering/Collaborative Innovation Center of Advanced Microstructures, Nanjing University, Nanjing, 210093, China

d. School of Physical Science and Technology, Ningbo University, 315211 Ningbo, China

E-mail addresses: xuezhaguo@buaa.edu.cn (Z. Xue); yulinwei@nju.edu.cn (L. Yu); pere.roca@polytechnique.edu (P. Roca i Cabarrocas)

Abstract

Silicon nanowires (SiNWs) are advantageous building blocks to explore a wide range of high performance nanoelectronics and photonics devices. In-plane solid-liquid-solid (IPSLS) SiNWs, grown by metal catalyst droplets that absorb hydrogenated amorphous silicon (a-Si:H) thin film to produce crystalline SiNWs, are particularly suitable for planar device fabrication and integration. Here, we explore a new growth control dimension to tailor the geometry of the in-plane SiNWs from island-chain to zigzag and to straight morphologies by using a simple plasma modification of the a-Si:H thin film precursor. This unique capability is due to the fact that the Gibbs energy and bonding status of the a-Si:H layer can be largely modified by the plasma treatments at various substrate temperatures, which in turn have a huge impact on the growth balance condition of the SiNWs and consequently on their morphologies. These results highlight a facile and yet highly effective strategy to tailor the morphology of in-plane SiNWs that will find important applications in fabricating nanoelectronic, sensor and logic devices.

Keywords: in-plane nanowires, plasma treatment, a-Si:H Gibbs energy, morphology engineering, in-plane solid-liquid-solid interface

1. Introduction

Silicon nanowires (SiNWs) with controllable morphologies are ideal building blocks to explore various novel nanoelectronic devices[1-7], where periodic diameter or orientation self-oscillations provide unique routes to tailor the desired photonic, transport, and mechanical properties targeting at specific optoelectronics[8-12], quantum electronics[13-16], flexible/stretchable electronics[17-21], and bioelectronics applications[22-24]. So far, pioneering studies have been devoted to tailor the morphologies of SiNWs via “top-down” or “bottom-up” approaches. For example, diameter modulated SiNWs can be etched out of uniform SiNWs encoded with complex doping profiles along the growth axis[25]; self-assembled vertical kinked SiNWs have been grown by applying alternative purge/and chamber pressure variation cycles during a vapor–liquid–solid (VLS) growth process[26-28]; confinement-guided[29] and line-shape programming[30-32] have been used to grow VLS SiNWs in pre-defined pattern channels or guiding edges. Recently, we have discovered an in-plane solid-liquid-solid (IPSLS) growth mode, where metal droplets are used to absorb an a-Si:H layer and produce crystalline SiNWs[33-36]. During this course, the advance rates of the front liquid/a-Si:H absorption and the rear liquid/SiNW deposition interfaces can be tuned by the ratio of droplet size over a-Si:H layer thickness, and thus tailor the geometry of the as-grown SiNWs to vary in a controlled way from island-chain, to straight and zigzag[37, 38]. However, the impact of the Gibbs energy of the a-Si:H feeding layer on the growth dynamics of in-plane SiNWs has never been explored, which could represent a new, as well as more convenient and effective parameter to achieve a programmable morphology engineering.

Meanwhile, plasma surface modification is a widely used technology that has been introduced to optimize the surface properties of various thin films[39-45], e.g. to improve interface passivation in various crystalline silicon solar cells[46-50], and to relax the constraints of the conductivity/transparency trade-off in ZnO thin films[51]. Here, we demonstrate a new strategy to modify the Gibbs energy

of the a-Si:H thin film precursor, specifically the density of bonded hydrogen and the degree of disorder in a-Si:H, which allows to efficiently engineer the morphology of Sn-catalyzed in-plane SiNWs from island-chain, to zigzag and straight, as seen in Fig. 1. This new strategy, based on a combination of plasma treatments of the a-Si:H thin film at various temperatures, can help to modify the Gibbs energy of the a-Si:H thin film precursor, and as a consequence to control the morphology of in-plane SiNWs. This opens a whole new control strategy to tailor the morphology of SiNWs, which is a key capability required to promote their application as the building blocks for the next generation of Si-based nanoelectronic devices.

2. Morphology control via a-Si:H modification

2.1 Experiments

In-plane SiNWs were grown on Si substrates with pre-patterned ~30nm Sn pads in a plasma-enhanced chemical vapor deposition (PECVD) system[33-35, 37, 38, 52]. The fabrication process can be divided into four steps as schematically illustrated in Fig. 1: (a) Hydrogen plasma treatment of Sn pads (40 nm in thickness) at 250°C to reduce the native Sn oxide layer and form discrete Sn catalyst droplets with a mean diameter of ~300nm (Fig. S1); (b) Deposition of a-Si:H thin film with a thickness of ~25nm at 120 °C; (c) a-Si:H thin film modification; and (d) annealing at 400°C to activate the growth of in-plane SiNWs. Depending on the a-Si:H modification conditions, different morphologies of SiNWs can be obtained as shown in Fig. 1e to 1l.

In our previous works, a-Si:H layer thickness has been used as the major parameter to control the morphology of the in-plane SiNWs growth, led by Sn droplets[32, 37, 38], where the chemical or Gibbs energy of a-Si:H layer was always fixed. In this work, we focus on the use of H₂ or Ar gas plasma treatments at various substrate temperatures to modify the chemical and structural properties of the a-Si:H thin film. The scanning electron microscopy (SEM) images of the as-grown SiNWs with different plasma treatment conditions are shown in Fig. 1e-1l. It is very clear that the morphologies of the produced in-plane SiNWs can

be significantly modified by the plasma treatment of the a-Si:H layer. Specifically, for H₂ plasma (HP) treatment, the low temperature treatment of a-Si:H at ~120 °C (Fig. 1e and 1f) produces long island-chain SiNWs, with length distribution of the island-chain SiNWs shown in Fig. 3b, while a higher temperature (~270-400°C) HP treatment (Fig. 1g and 1h) changes SiNWs into zigzag growth mode. In contrast, the Argon plasma (AP) treatment of a-Si:H at low temperature (~120°C) causes a similar zigzag growth mode, but simultaneously with shorter SiNW length and less self-turning periods, while a higher temperature AP treatment of the a-Si:H caused the catalyst to grow into very straight lines.

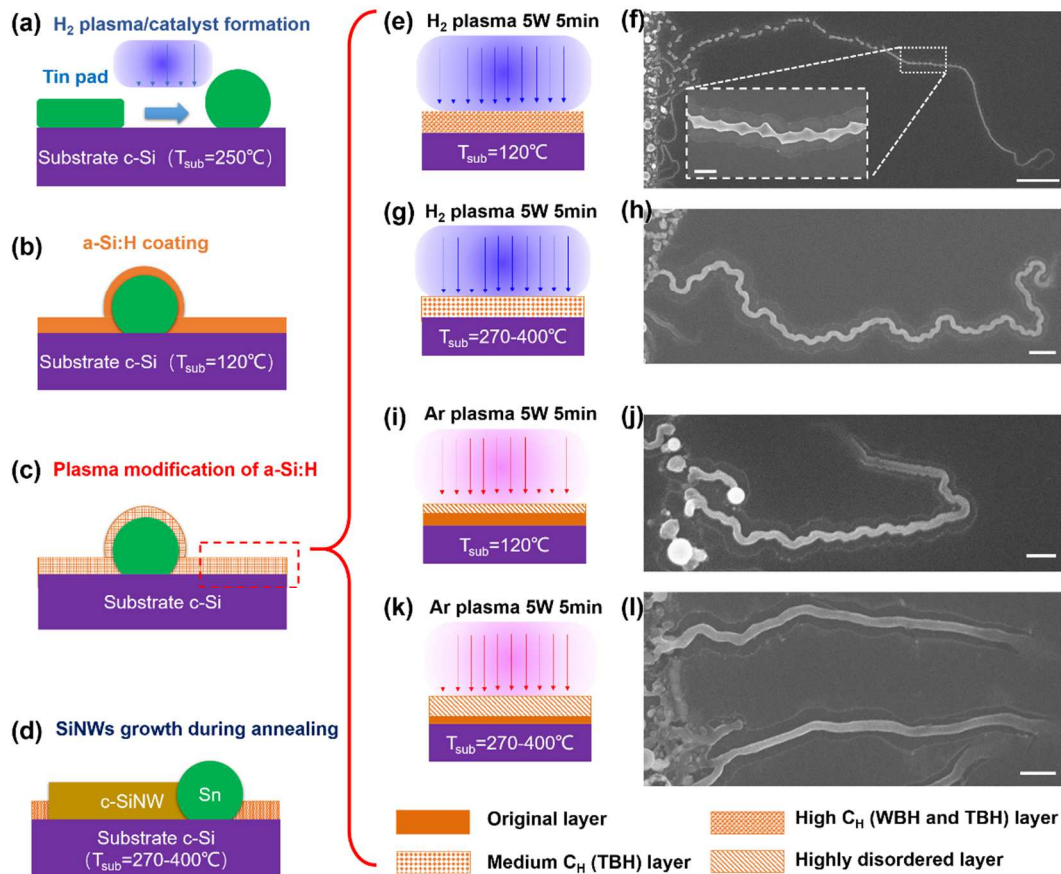


Fig. 1 Fabrication procedure for precise control of in-plane SiNW morphology via various plasma treatments of the a-Si:H precursor. (a-d) schematic illustration of the key process of in-plane SiNW growth, (a) H₂ plasma treatment of the Sn pad, (b) a-Si:H deposition, (c) a-Si:H modification, (d) annealing to grow in-plane SiNWs; (e), (g), (i) and (k) are four different process conditions for a-Si:H modification, leading to controlled growth of in-plane SiNW morphologies; (f), (h), (j) and (l) are the SEM images of in-plane SiNW morphologies as-grown via various plasma treatments of the a-Si:H precursor, from diameter-modulated island-chain growth mode (f), to self-turning zigzag growth mode ((h) and (j)), and to straight growth mode (l). Scale bars are 2 μm in (f), 200nm in inset of (f), 500nm in (h), (j) and (l).

2.2 Discussion of the growth modes

In general, the dissolved Si atoms within a running Sn catalyst droplet will diffuse from the higher concentration region (the front interface in contact with the a-Si:H thin film precursor) to the lower concentration region (the deposition interface in contact with growing SiNW), as shown in Fig. 2a, which is the key driving force for the catalyst droplet to absorb more Si atoms continuously from the a-Si:H front interface and to precipitate c-SiNWs at the rear, with the reduction of Gibbs energy from the amorphous (G_a) to crystalline (G_0) phases, $\Delta G = G_a - G_0$ (Fig. 2b). Obviously, the Gibbs energy of a-Si:H (G_a) is the key parameter that determines the driving force for the in-plane movement of the catalyst droplets and the SiNWs growth. Meanwhile, the plasma treatment of a-Si:H in Fig. 1 mainly modifies the state of a-Si:H, expressed in terms of Gibbs energy. Thus, a higher Gibbs energy of the a-Si:H thin film establishes a higher local equilibrium concentration of the dissolved Si atoms at the front a-Si:H/Sn absorption interface (C_{aSi}), with respect to that established at the rear Sn/c-Si deposition or growth interface (C_0) with a relation of $C_{aSi} = e^{\Delta G/kT} C_0$.

As sketched in Fig. 2c, the difference of the equilibrium concentrations at the front and at the rear interfaces will drive diffusion of the dissolved Si atoms across the droplet and establish a supersaturation concentration C_{Si} at the rear interface. Once this supersaturation is established (that is, with $C_{Si} > C_0$), nucleation will happen and the dissolved Si atoms will attach continuously to the formed nucleation sites, with a rate of $R_{att} = B(C_{Si} - C_0)$, where B is a pre-factor constant. So the axial advance speed of the rear Sn/c-Si interface can be written as:

$$v_{dep} \sim R_{att} = B(C_{Si} - C_0), \quad (1)$$

In the meantime, the continuous absorption interface draws the catalyst droplet to move on forward, with an advancing speed determined by the diffusion transport of Si atoms through the catalyst droplet. Thus, the moving speed of the front absorption interface can be written as

$$v_{abs} \sim g_{diff} D_s (C_{aSi} - C_{Si}) / L_c, \quad (2)$$

where L_c , D_s and g_{diff} are the length of Sn droplet, the diffusion constant of Si atoms in Sn droplet and the geometric correction factor accounting for the asymmetric width of the front and rear interfaces, respectively.

As sketched in Fig. 2c and 2d, if C_{aSi} (G_{aSi}) increases, the droplet encounters a stronger driving force for absorption, and its front interface is pulled forward more intensely, leading to a stretched Sn catalyst droplet that tends to produce an island-chain structure under the Plateau-Rayleigh (PR) oscillation[38]. Otherwise, if C_{aSi} (G_{aSi}) reduces, the droplet encounters a weaker driving force at the front absorption interface, and thus the droplet will be squeezed to produce a zigzag NW. Therefore, we could draw the following conclusions:

$$C_{aSi}^{island-chain} > C_{aSi}^0 > C_{aSi}^{zigzag} \quad (3)$$

$$G_{aSi}^{island-chain} > G_{aSi}^0 > G_{aSi}^{zigzag} \quad (4)$$

Based on this idea, the key control parameter adopted in this work is to adjust or modify the Gibbs energy of the a-Si:H precursor thin film, by using different plasma treatment conditions, which in turn provides a new dimension of control to engineer the morphology of the as-grown in-plane SiNWs.

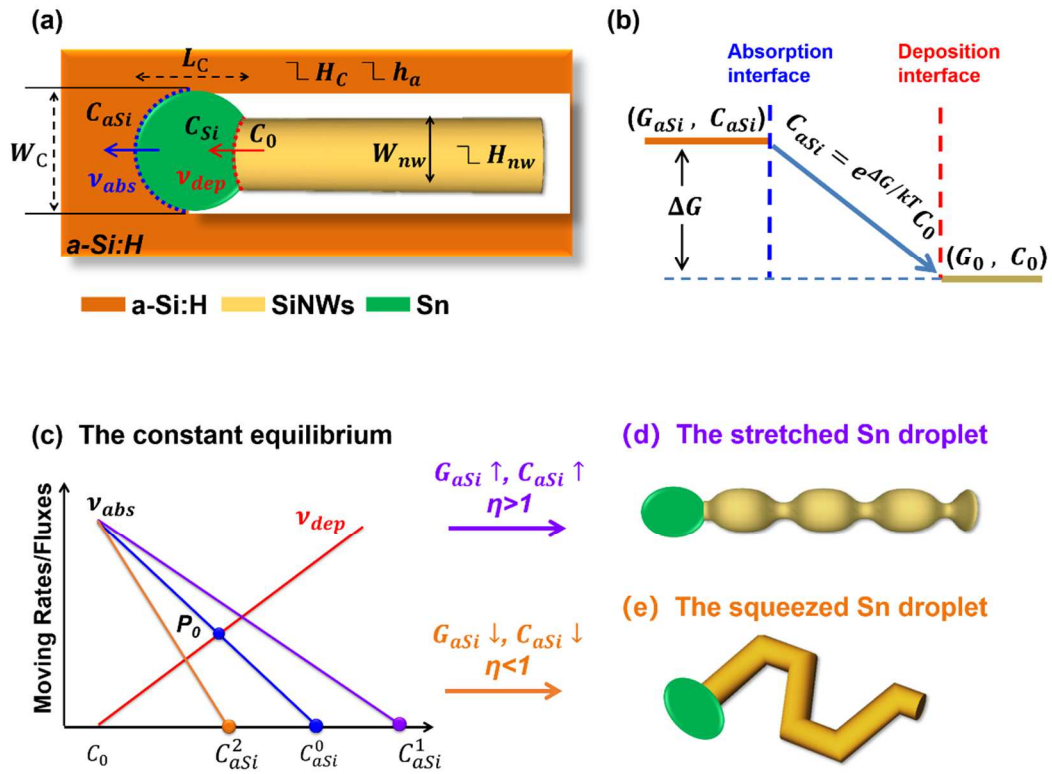


Fig. 2 The growth modes of different morphologies of in-plane SiNWs. (a) illustrates the key parameters of in-plane SiNWs growth, where the height of the SiNW and the Sn droplet, and the thickness of the a-Si:H layer are labeled as H_{nw} , H_C and h_a , respectively; (b) Schematic illustration for the relative Gibbs energy of Si atoms in the crystalline SiNW, Sn catalyst droplet, and a-Si:H thin film. (c-d) delineates the growth modes determined by equilibrium concentration of dissolved Si atoms at the front a-Si:H/Sn absorption interface (C_{aSi}). The blue (red) lines represent the evolution trend of the front absorption (rear deposition) rate as a function of the dissolved Si atom concentration C_{Si} , and the insets present the stretched or squeezed Sn droplet in the corresponding growth mode.

3. Hydrogen effusion measurements of a-Si:H

The effect of hydrogen in a-Si:H thin films has been a fundamental research topic that has attracted tremendous interests and efforts since the 80's of last century[53-57], where the evolution of the densities of defects, voids and weakly dangling bonded hydrogen in a-Si:H are mediated by the locations and motion of hydrogen atoms (e.g. hydrogen incorporation, diffusion and release)[58]. All these factors could contribute to the change of Gibbs energy in a-Si:H (G_a), which could break down into $G_a = G_{BH} + G_{disorder} + G_{other}$, with the contribution of bonded hydrogen (G_{BH}), the disorder, defects, and voids ($G_{disorder}$) and other factors (G_{other}) (e.g. the interface energy).

To characterize the effect of the plasma treatments on the a-Si:H thin film precursor, hydrogen effusion measurements were conducted[59], where hydrogen released from thin film was detected by a quadrupole mass spectrometer (QMS) . The hydrogen effusion system consists of a furnace connected to a QMS (Prisma™ 80 set) to measure the evolution of effusing molecular hydrogen as a function of temperature during the annealing from room temperature (RT) to 700°C (10°C/min) in a high vacuum. We deposited 9 samples of ~25 nm of a-Si:H (as deduced from the analysis of spectroscopic ellipsometry measurements) on c-Si substrates, and then exposed them to different processes and plasma treatments, as described in detail in Experimental methods and summarized in Table S1. Then, these samples were characterized by gas evolution measurements. The entire system is kept under pumping a high vacuum at 4×10^{-7} mbar. The hydrogen effusion plots of these nine samples, normalized to the volume of a-Si:H, are shown in Fig. 3c, 4a, 5a for comparative study, respectively.

3.1 a-Si:H modification by H₂ plasma treatment

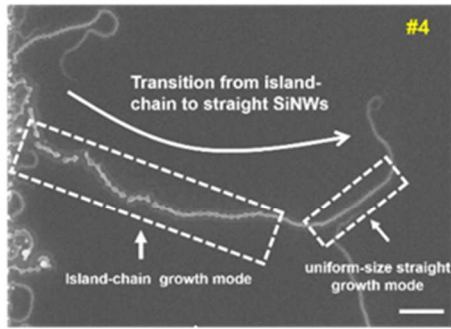
As shown in Fig. 3c, sample #1 (the reference a-Si:H) has two main effusion stages termed low (LT, ~300°C) and high (HT, ~385°C) temperature, corresponding to the weakly bonded hydrogen (WBH) and the tightly bonded hydrogen (TBH), respectively[55, 56]. Then, for sample #2, where the as-deposited a-Si:H was heated to 400°C and kept for 1min to reproduce in-plane SiNWs growth conditions, the LT peak (WBH density) is observed to decrease significantly by ~41%, while the HT peak (TBH density) also decreases but not so much only ~18%, which can be understood as the normal phenomenon of the hydrogen effusion out of a-Si:H thin film during the annealing taking place during the SiNW growth step at 400 °C in the PECVD system(seen Fig. 1d). So, samples #1 and #2 here are used as the references to compare the changes of plasma modified a-Si:H.

To understand HP treatment at low temperature (120°C), hydrogen effusion curves of sample #3 and #4 are plotted in Fig. 3c. Interestingly, for sample #3, the hydrogen effusion peak at 300°C (LT peak, WBH) strongly increases compared to that of sample #1, indicating that the HP treatment at low

temperature would react and introduce hydrogen atoms into the a-Si:H network[60, 61]. Meanwhile, adding the 400 °C annealing for 1 min (i.e. sample #4) leads to a higher LT peak (WBH density) than that of sample #2, implicating that a portion of the injected hydrogen atoms has been redistributed among the a-Si:H matrix during the 400 °C annealing. What is more, we find that, the yield and length of island-chain SiNWs growth can be significantly increased, while there is no observation of the zigzag growth mode, as witnessed in Fig. 3a, 3b and Fig. S2. The statistical data (Fig. S3) also shows that the HP treatment substantially increases the percentage of the island-chain part (from 40% to 80%) in the total length of SiNWs.

Considering the results in Fig. 3 and Fig. S3, it can be inferred that it is the much higher density of WBH that increases the Gibbs energy of a-Si:H (G_{BH} increases, so G_a increases), which leads to a stretching dynamics of the leading Sn catalyst droplet to produce island-chain due to the Plateau-Rayleigh (PR) oscillation[38]. It is also the reason why the strong increase of WHB affects for a longer time the PR oscillation and maintains a more extended length of island-chain growth (Fig. 3a and 3b), before transforming into straight growth mode, associated to the decrease of Gibbs energy of a-Si:H[37, 38].

(a) The morphology of in-plane SiNW



(c) Hydrogen Exodiffusion spectrum

No.	Thickness	Treatment conditions
#1	28nm	Reference= as deposited at 120°C, 5W, SiH ₄ 0.1Torr, 5min
#2	29nm	#1 + anneal at 400°C H ₂ 1Torr 1min
#3	30nm	#1 + H ₂ plasma at 120°C 5W, 1Torr, 5min
#4	26nm	#3 + annealed at 400°C, H ₂ 1Torr, 1min

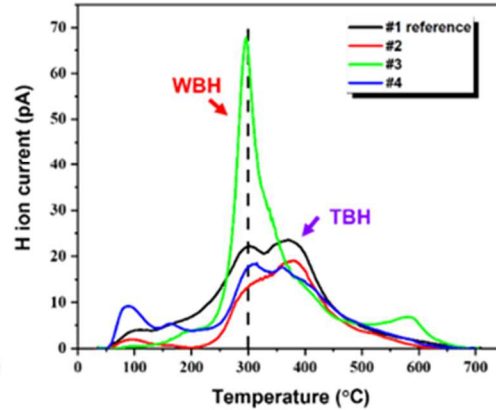
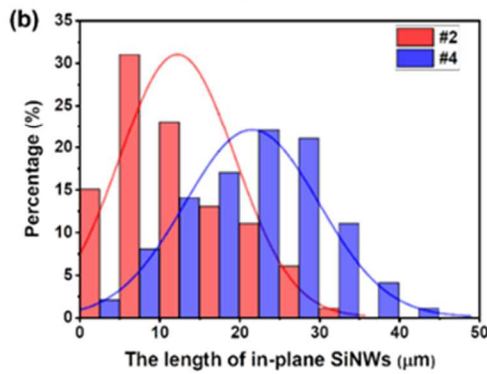
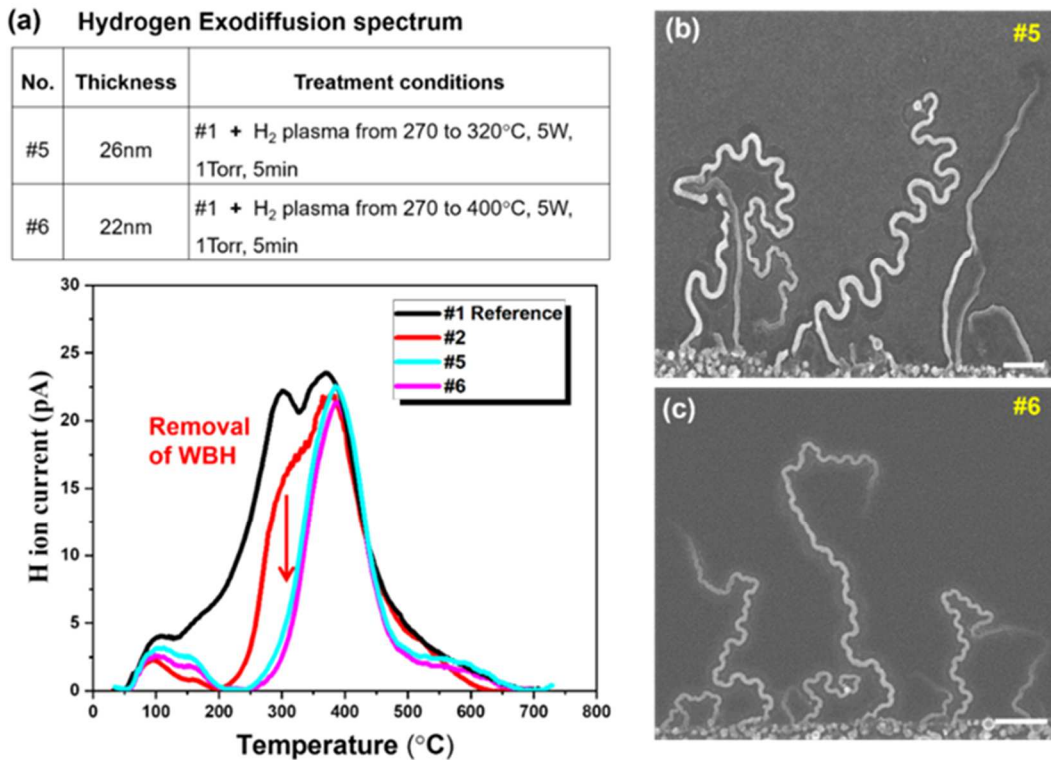


Fig. 3 In-plane island-chain SiNWs growth. (a) typical SEM image of Sn-mediated in-plane SiNWs as-grown after a H₂ plasma treatment at 120°C, starting with an island-chain growth mode followed by straight growth mode. Scale bar is 2μm. (b) the comparison of the length distribution of in-plane island-chain SiNWs as-grown with and without H₂ plasma treatment at 120°C. (c) Normalized hydrogen exodiffusion evolution ion current as a function of temperature for four different processes with the conditions indicated by the labels of the plots in the top table.

On the other hand, considering the in-plane zigzag SiNWs are grown with a lower Gibbs energy of a-Si:H, the Plateau-Rayleigh oscillation of Sn droplets will be suppressed. From the above results, we expect to reduce the Gibbs energy by removing WBH thanks to a high temperature plasma treatment before in-plane SiNWs growth. In-situ SEM studies of in-plane SiNWs growth[33, 37] inform that Sn catalyzed growth starts from about 270°C at the rate of several nm/s, so the high temperature plasma treatment should start at 270°C, to avoid missing the initial growth during temperature increase.

As shown by the H⁺ ion current profiles of samples #5 and #6 in Fig. 4a, HP treatment at high temperature (>300°C) does remove WBH from the a-Si:H thin film. This is because high temperature HP could be able to react and re-arrange the a-Si network, working as chemical annealing [44, 62-65]. Thus the bonded hydrogen term of the Gibbs energy G_{BH} decreases and so does G_a at the same

time. Accordingly, due to the removal of WBH and the reduction of G_a , there is no island-chain growth of the as-grown SiNWs in Fig. 4b, 4c and Fig. S4,



corresponding to the treatment of #5 and #6.

Fig. 4 In-plane zigzag SiNWs growth mode via H₂ plasma treatment at high temperature. (a) Normalized hydrogen exo-diffusion evolution ion current as a function of temperature for different processes with the conditions indicated by the labels of the plots in the top table. (b)-(c) typical SEM images of Sn-mediated in-plane SiNWs with the conditions indicated by the labels of the plots in (a); the scale bars are 1 μ m.

3.2 a-Si:H modification by Ar plasma treatment

In comparison, Ar plasma treatment leads to another kind of a-Si:H thin film modification, as the Ar atoms do not react with a-Si:H. However bombardment by Ar ions can damage the a-Si:H surface via the breaking of Si-Si and Si-H bonds, thus making the a-Si:H network more disordered. For the low temperature treatment, a higher degree of disorder promotes the out-diffusion of the hydrogen atoms from the a-Si:H matrix and accelerates the H elimination during high temperature annealing. Then, the LT peak ($\sim 300^\circ\text{C}$ WBH) in the H effusion evolution is wholly removed after AP treatment at 120°C and subsequent annealing at 400°C for 1min, as shown in the plot of #8 in Fig. 5a. Following the

more disorder and removal of WBH in a-Si:H thin film, Sn catalyst droplet will tend to be squeezed to produce zigzag SiNWs, as presented in Fig. 5b and Fig. S5.

In addition, the high temperature AP treatment can completely remove WBH peaks, as well as reduce the TBH, as shown in plot #9, while making a-Si:H more disordered. As a result, Sn catalyst droplet will be drawn by the front absorption interface to produce straight SiNWs, as witnessed in Fig. 5c and and Fig. S5.

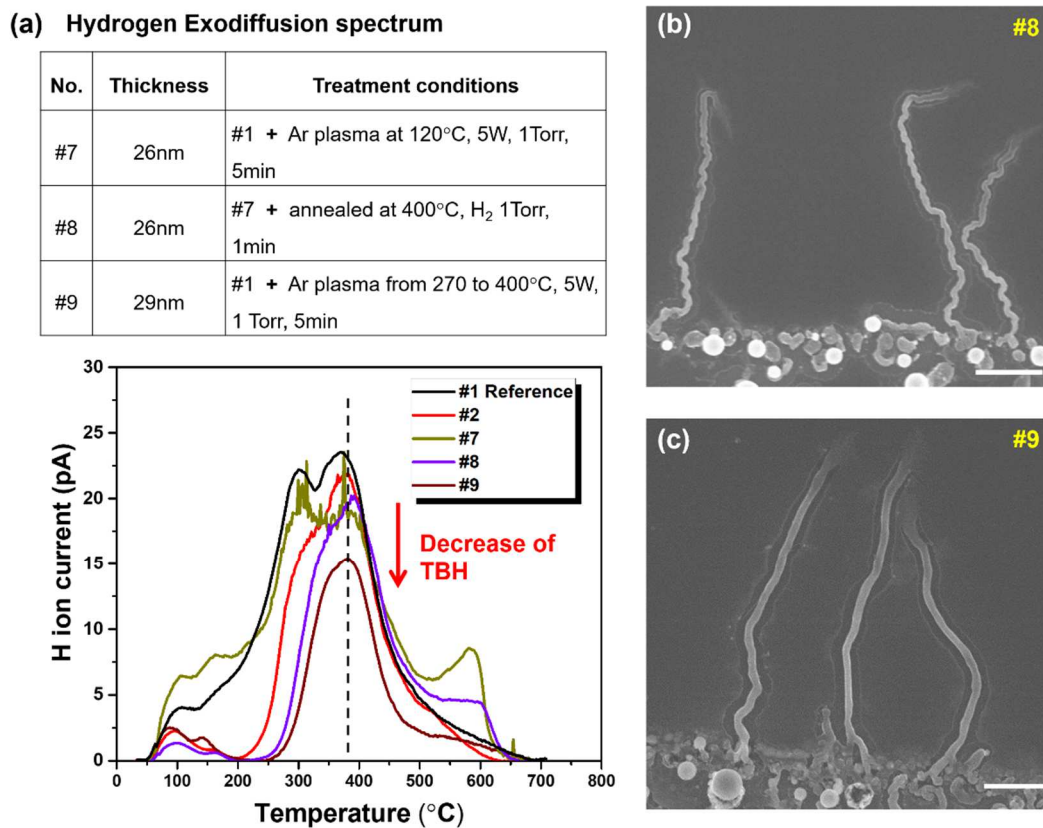


Fig. 5 In-plane straight SiNWs growth mode via Ar plasma treatment. (a) Normalized hydrogen exo-diffusion evolution ion current as a function of temperature for different processes with the conditions indicated by the labels of the plots in the top table; (b) and (c) the typical SEM images of Sn-mediated in-plane SiNWs with Ar plasma treatment at low temperature(b) and high temperature(c); the scale bars are 1 μ m.

In particular, the amplitude of hydrogen exo-diffusion peak at 385°C decreases as the degree of disorder increases, from sample #5 and #6 to #8 and #9 as clearly shown in Fig. S6a. Interestingly, the amplitude angle (θ) and period length (L_p) of self-turning in-plane zigzag SiNW springs also decrease, and eventually, the as-grown SiNWs become straight as shown in Fig. 5c. The comparison of this

quantitative change is presented in Fig. S6b-g. Based on the discussion above, we can reasonably conclude that the Gibbs energy of sample #4, #7, #8 and #9 in Fig. 1e, 1g, 1i, 1k satisfies the following relation:

$$G_a^{\#4} > G_a^{ref} > G_a^{\#9} > G_a^{\#8} > G_a^{\#6} > G_a^{\#5},$$

which is also consistent with the growth mode of as-grown in-plane SiNW morphology.

4. Conclusions

In summary, we have demonstrated a new strategy for in-plane SiNWs growth via plasma modification of the a-Si:H thin film precursor. This strategy allows us to precisely tailor the morphology of Sn-catalyzed in-plane SiNWs, from the diameter-modulated island-chain, to the self-turning zigzag, and to straight geometries, while the a-Si:H layer thickness was kept constant. These unique morphology control capabilities derive from the effective plasma treatments that modify substantially the density and distribution of the bonded hydrogen and the degree of disorder in a-Si:H, which results in changed Gibbs energy in the precursor layer. These results emphasize a completely new morphology control dimension for the planar growth of SiNWs and could eventually provide an unprecedented opportunity to tailor and batch-manufacture more complex and functional nanostructures and devices.

5. Experimental methods

Samples for hydrogen effusion measurements: **#1:** as-deposited a-Si:H reference sample; **#2:** heating up under vacuum to 400 °C and annealed for 1 min to reproduce the conditions of SiNWs growth; **#3:** H₂ plasma treatment (HPT) under a RF power of 5 W (the RF power density is 22.2 mW/cm²) for 5 min under a pressure of 1 Torr at 120 °C; **#4:** the same HPT as #3, and then increasing the temperature to 400 °C to stay for 1 min; **#5:** increasing the temperature to 320 °C while exposing to a 5 W HPT under a pressure of 1 Torr starting at 270 °C (this heating process from 270 to 320 °C takes 2 min) and holding the sample at 320

°C for 3 min (the total HPT time is 5 min); **#6**: increasing the temperature to 400 °C while exposing to H₂ plasma of 5 W under a pressure of 1 Torr starting at 270 °C and holding at 400 °C for 1min (the total HPT time is also 5min); **#7**: Ar plasma treatment (APT) at 120 °C under a pressure of 1Torr 5W for 5min; **#8**: same APT as #7, and then increasing the temperature to 400 °C to hold on for 1min; **#9**: increasing temperature to 400 °C and APT 5W under a pressure of 1Torr starting at 270 °C and hold at 400 °C for 1min (totally 5min).

CRedit authorship contribution statement

Zhaoguo Xue: Conceptualization, Methodology, Validation, Formal analysis, Writing - Original Draft, Investigation, Visualization, Writing – review & editing, Funding acquisition. **Wanghua Chen**: Methodology, Formal analysis, Writing - Review & Editing, Funding acquisition. **Xianhong Meng**: Methodology, Writing - Review & Editing, Resources, Funding acquisition. **Jun Xu**: Resources, Writing - Review & Editing. **Yi Shi**: Resources, Writing - Review & Editing. **Kunji Chen**: Resources, Writing - Review & Editing. **Linwei Yu**: Supervision, Conceptualization, Methodology, Writing - Review & Editing, Project administration, Funding acquisition. **Pere Roca i Cabarrocas**: Supervision, Conceptualization, Methodology, Writing - Review & Editing, Resources, Project administration.

Declaration of Competing Interest

The authors declare that they have no known competing financial interests or personal relationships that could have appeared to influence the work reported in this paper.

Acknowledgements

This work was supported by the National Natural Science Foundation of China under Nos. 11874198, 61904095 and 12172027, National Postdoctoral Program for Innovative Talents under No. BX20180157, China Postdoctoral Science Foundation under No. 2018M641333, and the Natural Science Foundation of Ningbo, China under No. 2021J068.

References

- [1] C. Jia, Z. Lin, Y. Huang, X. Duan, Nanowire Electronics: From Nanoscale to Macroscale, *Chem. Rev.*, 119 (2019) 9074-9135. <https://doi.org/10.1021/acs.chemrev.9b00164>
- [2] N.P. Dasgupta, J. Sun, C. Liu, S. Brittman, S.C. Andrews, J. Lim, H. Gao, R. Yan, P. Yang, 25th anniversary article: semiconductor nanowires--synthesis, characterization, and applications, *Adv. Mater.*, 26 (2014) 2137-2184. <https://doi.org/10.1002/adma.201305929>
- [3] A. Zhang, C.M. Lieber, Nano-Bioelectronics, *Chem. Rev.*, 116 (2016) 215-257. <https://doi.org/10.1021/acs.chemrev.5b00608>
- [4] V. Schmidt, J.V. Wittemann, S. Senz, U. Gösele, Silicon Nanowires: A Review on Aspects of their Growth and their Electrical Properties, *Adv. Mater.*, 21 (2009) 2681-2702. <https://doi.org/10.1002/adma.200803754>
- [5] L. Baraban, B. Ibarlucea, E. Baek, G. Cuniberti, Hybrid Silicon Nanowire Devices and Their Functional Diversity, *Adv. Sci.*, 6 (2019) 1900522. <https://doi.org/10.1002/advs.201900522>
- [6] Y. Jiang, B. Tian, Inorganic semiconductor biointerfaces, *Nat. Rev. Mater.*, 3 (2018) 473-490. <https://doi.org/10.1038/s41578-018-0062-3>
- [7] I.M.A. Fontcuberta, Nanostructured alloys light the way to silicon-based photonics, *Nature*, 580 (2020) 188-189. <https://doi.org/10.1038/d41586-020-00976-8>
- [8] R.W. Day, M.N. Mankin, R. Gao, Y.S. No, S.K. Kim, D.C. Bell, H.G. Park, C.M. Lieber, Plateau-Rayleigh crystal growth of periodic shells on one-dimensional substrates, *Nature Nanotech.*, 10 (2015) 345-352. <https://doi.org/10.1038/nnano.2015.23>
- [9] R.W. Day, M.N. Mankin, C.M. Lieber, Plateau-Rayleigh Crystal Growth of Nanowire Heterostructures: Strain-Modified Surface Chemistry and Morphological Control in One, Two, and Three Dimensions, *Nano Lett.*, 16 (2016) 2830-2836. <https://doi.org/10.1021/acs.nanolett.6b00629>
- [10] Y. Li, F. Qian, J. Xiang, C.M. Lieber, Nanowire electronic and optoelectronic devices, *Mater. Today*, 9 (2006) 18-27. [https://doi.org/10.1016/s1369-7021\(06\)71650-9](https://doi.org/10.1016/s1369-7021(06)71650-9)
- [11] R.J. Chen, D.H. Li, H.L. Hu, Y.Y. Zhao, Y. Wang, N. Wong, S.J. Wang, Y. Zhang, J. Hu, Z.X. Shen, Q.H. Xiong, Tailoring Optical Properties of Silicon Nanowires by Au Nanostructure Decorations: Enhanced Raman Scattering and Photodetection, *J. Phys. Chem. C*, 116 (2012) 4416-4422. <https://doi.org/10.1021/jp210198u>
- [12] A.D. Mallorqui, E. Alarcon-Llado, I.C. Mundet, A. Kiani, B. Demareux, S. De Wolf, A. Menzel, M. Zacharias, A.I. Morral, Field-effect passivation on silicon nanowire solar cells, *Nano Res.*, 8 (2015) 673-681. <https://doi.org/10.1007/s12274-014-0551-7>
- [13] F.A. Zwanenburg, A.S. Dzurak, A. Morello, M.Y. Simmons, L.C.L. Hollenberg, G. Klimeck, S. Rogge, S.N. Coppersmith, M.A. Eriksson, Silicon quantum electronics, *Rev. Mod. Phys.*, 85 (2013) 961-1019. <https://doi.org/10.1103/RevModPhys.85.961>
- [14] F.A. Zwanenburg, C.E. van Rijmenam, Y. Fang, C.M. Lieber, L.P. Kouwenhoven, Spin states of the first four holes in a silicon nanowire quantum dot, *Nano Lett.*, 9 (2009) 1071-1079. <https://doi.org/10.1021/nl803440s>
- [15] S. Lee, Y. Lee, E.B. Song, T. Hiramoto, Modulation of peak-to-valley current ratio of Coulomb blockade oscillations in Si single hole transistors, *Appl. Phys. Lett.*, 103 (2013) 103502. <https://doi.org/10.1063/1.4819442>
- [16] K.S. Yi, K. Trivedi, H.C. Floresca, H. Yuk, W. Hu, M.J. Kim, Room-temperature quantum confinement effects in transport properties of ultrathin Si nanowire field-effect transistors, *Nano Lett.*, 11 (2011) 5465-5470. <https://doi.org/10.1021/nl203238e>
- [17] S.Y. Ryu, J. Xiao, W.I. Park, K.S. Son, Y.Y. Huang, U. Paik, J.A. Rogers, Lateral buckling mechanics in silicon nanowires on elastomeric substrates, *Nano Lett.*, 9 (2009) 3214-3219. <https://doi.org/10.1021/nl901450q>
- [18] F. Xu, W. Lu, Y. Zhu, Controlled 3D buckling of silicon nanowires for stretchable electronics, *ACS Nano*, 5 (2011) 672-678. <https://doi.org/10.1021/nn103189z>
- [19] L. Wang, K. Zheng, Z. Zhang, X. Han, Direct atomic-scale imaging about the mechanisms of ultralarge bent straining in Si nanowires, *Nano Lett.*, 11 (2011) 2382-2385. <https://doi.org/10.1021/nl200735p>
- [20] K. Zheng, X. Han, L. Wang, Y. Zhang, Y. Yue, Y. Qin, X. Zhang, Z. Zhang, Atomic mechanisms governing the elastic limit and the incipient plasticity of bending Si nanowires, *Nano Lett.*, 9 (2009) 2471-2476. <https://doi.org/10.1021/nl9012425>
- [21] Z. Xue, H. Song, J.A. Rogers, Y. Zhang, Y. Huang, Mechanically-Guided Structural Designs

- in Stretchable Inorganic Electronics, *Adv. Mater.*, 32 (2020) e1902254. <https://doi.org/10.1002/adma.201902254>
- [22] B. Tian, T. Cohen-Karni, Q. Qing, X. Duan, P. Xie, C.M. Lieber, Three-dimensional, flexible nanoscale field-effect transistors as localized bioprobes, *Science*, 329 (2010) 830-834. <https://doi.org/10.1126/science.1192033>
- [23] Q. Qing, Z. Jiang, L. Xu, R. Gao, L. Mai, C.M. Lieber, Free-standing kinked nanowire transistor probes for targeted intracellular recording in three dimensions, *Nature Nanotech.*, 9 (2014) 142-147. <https://doi.org/10.1038/nnano.2013.273>
- [24] B. Tian, C.M. Lieber, Nanowired Bioelectric Interfaces, *Chem. Rev.*, 119 (2019) 9136-9152. <https://doi.org/10.1021/acs.chemrev.8b00795>
- [25] J.D. Christesen, C.W. Pinion, E.M. Grumstrup, J.M. Papanikolas, J.F. Cahoon, Synthetically Encoding 10 nm Morphology in Silicon Nanowires, *Nano Lett.*, 13 (2013) 6281-6286. <https://doi.org/10.1021/nl403909r>
- [26] B. Tian, P. Xie, T.J. Kempa, D.C. Bell, C.M. Lieber, Single-crystalline kinked semiconductor nanowire superstructures, *Nature Nanotech.*, 4 (2009) 824-829. <https://doi.org/10.1038/nnano.2009.304>
- [27] Z. Jiang, Q. Qing, P. Xie, R. Gao, C.M. Lieber, Kinked p-n Junction Nanowire Probes for High Spatial Resolution Sensing and Intracellular Recording, *Nano Lett.*, 12 (2012) 1711-1716. <https://doi.org/10.1021/nl300256r>
- [28] L. Xu, Z. Jiang, Q. Qing, L. Mai, Q. Zhang, C.M. Lieber, Design and synthesis of diverse functional kinked nanowire structures for nanoelectronic bioprobes, *Nano Lett.*, 13 (2013) 746-751. <https://doi.org/10.1021/nl304435z>
- [29] A. Pevzner, Y. Engel, R. Elnathan, A. Tsukernik, Z. Barkay, F. Patolsky, Confinement-guided shaping of semiconductor nanowires and nanoribbons: "writing with nanowires", *Nano Lett.*, 12 (2012) 7-12. <https://doi.org/10.1021/nl201527h>
- [30] Z. Xue, M. Sun, T. Dong, Z. Tang, Y. Zhao, J. Wang, X. Wei, L. Yu, Q. Chen, J. Xu, Y. Shi, K. Chen, P. Roca i Cabarrocas, Deterministic Line-Shape Programming of Silicon Nanowires for Extremely Stretchable Springs and Electronics, *Nano Lett.*, 17 (2017) 7638-7646. <https://doi.org/10.1021/acs.nanolett.7b03658>
- [31] T. Dong, Y. Sun, Z. Zhu, X. Wu, J. Wang, Y. Shi, J. Xu, K. Chen, L. Yu, Monolithic Integration of Silicon Nanowire Networks as a Soft Wafer for Highly Stretchable and Transparent Electronics, *Nano Lett.*, 19 (2019) 6235-6243. <https://doi.org/10.1021/acs.nanolett.9b02291>
- [32] Z. Xue, T. Dong, Z. Zhu, Y. Zhao, Y. Sun, L. Yu, Engineering in-plane silicon nanowire springs for highly stretchable electronics, *J. Semicond.*, 39 (2018). <https://doi.org/10.1088/1674-4926/39/1/011001>
- [33] L. Yu, P.J. Alet, G. Picardi, P. Roca i Cabarrocas, An in-plane solid-liquid-solid growth mode for self-avoiding lateral silicon nanowires, *Phys. Rev. Lett.*, 102 (2009) 125501. <https://doi.org/10.1103/PhysRevLett.102.125501>
- [34] L. Yu, P. Roca i Cabarrocas, Growth mechanism and dynamics of in-plane solid-liquid-solid silicon nanowires, *Phys. Rev. B*, 81 (2010). <https://doi.org/10.1103/PhysRevB.81.085323>
- [35] L. Yu, P. Roca i Cabarrocas, Initial nucleation and growth of in-plane solid-liquid-solid silicon nanowires catalyzed by indium, *Phys. Rev. B*, 80 (2009). <https://doi.org/10.1103/PhysRevB.80.085313>
- [36] Z. Fan, J.-L. Maurice, I. Florea, W. Chen, L. Yu, S. Guilet, E. Cambriil, X. Lafosse, L. Couraud, S. Bouchoule, P. Roca i Cabarrocas, In situ observation of droplet nanofluidics for yielding low-dimensional nanomaterials, *Appl. Surf. Sci.*, 573 (2022) 151510. <https://doi.org/https://doi.org/10.1016/j.apsusc.2021.151510>
- [37] Z.G. Xue, M.K. Xu, X. Li, J. Wang, X.F. Jiang, X.L. Wei, L.W. Yu, Q. Chen, J.Z. Wang, J. Xu, Y. Shi, K.J. Chen, P. Roca i Cabarrocas, In-Plane Self-Turning and Twin Dynamics Renders Large Stretchability to Mono-Like Zigzag Silicon Nanowire Springs, *Adv. Funct. Mater.*, 26 (2016) 5352-5359. <https://doi.org/10.1002/adfm.201600780>
- [38] Z. Xue, M. Xu, Y. Zhao, J. Wang, X. Jiang, L. Yu, J. Wang, J. Xu, Y. Shi, K. Chen, P. Roca i Cabarrocas, Engineering island-chain silicon nanowires via a droplet mediated Plateau-Rayleigh transformation, *Nat. Commun.*, 7 (2016) 12836. <https://doi.org/10.1038/ncomms12836>
- [39] S. Dou, L. Tao, R. Wang, S. El Hankari, R. Chen, S. Wang, Plasma-Assisted Synthesis and Surface Modification of Electrode Materials for Renewable Energy, *Adv. Mater.*, 30 (2018) e1705850. <https://doi.org/10.1002/adma.201705850>
- [40] P. Chu, Plasma-surface modification of biomaterials, *Materials Science and Engineering: R: Reports*, 36 (2002) 143-206. [https://doi.org/10.1016/s0927-796x\(02\)00004-9](https://doi.org/10.1016/s0927-796x(02)00004-9)
- [41] R. Morent, N. De Geyter, T. Desmet, P. Dubruel, C. Leys, Plasma Surface Modification of

- Biodegradable Polymers: A Review, *Plasma Processes and Polymers*, 8 (2011) 171-190. <https://doi.org/10.1002/ppap.201000153>
- [42] O.M. Slobodian, P.N. Okholin, P.M. Lytvyn, S.V. Malyuta, O.Y. Khyzhun, A.V. Vasin, A.V. Rusavsky, Y.V. Gomeniuk, V.I. Glotov, T.M. Nazarova, O.I. Gudymenko, A.N. Nazarov, Plasma treatment as a versatile tool for tuning of sorption properties of thin nanoporous carbon films, *Appl. Surf. Sci.*, 544 (2021) 11. <https://doi.org/10.1016/j.apsusc.2020.148876>
- [43] S. Nunomura, I. Sakata, K. Matsubara, Plasma-Induced Electronic Defects: Generation and Annihilation Kinetics in Hydrogenated Amorphous Silicon, *Physical Review Applied*, 10 (2018) 054006. <https://doi.org/10.1103/PhysRevApplied.10.054006>
- [44] S. Sriraman, S. Agarwal, E.S. Aydil, D. Maroudas, Mechanism of hydrogen-induced crystallization of amorphous silicon, *Nature*, 418 (2002) 62-65. <https://doi.org/10.1038/nature00866>
- [45] A. Neumüller, O. Sergeev, M. Vehse, C. Agert, Structural characterization of the interface structure of amorphous silicon thin films after post-deposition argon or hydrogen plasma treatment, *Appl. Surf. Sci.*, 403 (2017) 200-205. <https://doi.org/https://doi.org/10.1016/j.apsusc.2017.01.188>
- [46] L. Zhang, W. Guo, W. Liu, J. Bao, J. Liu, J. Shi, F. Meng, Z. Liu, Investigation of positive roles of hydrogen plasma treatment for interface passivation based on silicon heterojunction solar cells, *J. Phys. D: Appl. Phys.*, 49 (2016). <https://doi.org/10.1088/0022-3727/49/16/165305>
- [47] A. Descocudres, L. Barraud, S. De Wolf, B. Strahm, D. Lachenal, C. Guérin, Z.C. Holman, F. Zicarelli, B. Demareux, J. Seif, J. Holovsky, C. Ballif, Improved amorphous/crystalline silicon interface passivation by hydrogen plasma treatment, *Appl. Phys. Lett.*, 99 (2011). <https://doi.org/10.1063/1.3641899>
- [48] S.S. Saseendran, M.C. Raval, A. Kottantharayil, Impact of Post-deposition Plasma Treatment on Surface Passivation Quality of Silicon Nitride Films, *IEEE J. Photovolt.*, 6 (2016) 74-78. <https://doi.org/10.1109/Jphotov.2015.2493369>
- [49] A. Soman, U. Nsofor, U. Das, T. Gu, S. Hegedus, Correlation between in Situ Diagnostics of the Hydrogen Plasma and the Interface Passivation Quality of Hydrogen Plasma Post-Treated a-Si:H in Silicon Heterojunction Solar Cells, *ACS Appl Mater Interfaces*, 11 (2019) 16181-16190. <https://doi.org/10.1021/acsami.9b01686>
- [50] Z.P. Wu, L.P. Zhang, R.F. Chen, W.Z. Liu, Z.F. Li, F.Y. Meng, Z.X. Liu, Improved amorphous/crystalline silicon interface passivation for silicon heterojunction solar cells by hot-wire atomic hydrogen during doped a-Si:H deposition, *Appl. Surf. Sci.*, 475 (2019) 504-509. <https://doi.org/10.1016/j.apsusc.2018.12.239>
- [51] L. Ding, S. Nicolay, J. Steinhäuser, U. Kroll, C. Ballif, Relaxing the Conductivity/Transparency Trade-Off in MOCVD ZnO Thin Films by Hydrogen Plasma, *Adv. Funct. Mater.*, 23 (2013) 5177-5182. <https://doi.org/10.1002/adfm.201203541>
- [52] Y. Sun, T.G. Dong, J.Z. Wang, J. Xu, K.J. Chen, P. Roca i Cabarrocas, L.W. Yu, Meandering growth of in-plane silicon nanowire springs, *Appl. Phys. Lett.*, 114 (2019). <https://doi.org/10.1063/1.5097429>
- [53] R.A. Street, Hydrogen chemical potential and structure of a-Si:H, *Phys. Rev. B*, 43 (1991) 2454-2457. <https://doi.org/10.1103/physrevb.43.2454>
- [54] W.M.M. Kessels, A.H.M. Smets, D.C. Marra, E.S. Aydil, D.C. Schram, M.C.M. van de Sanden, On the growth mechanism of a-Si:H, *Thin Solid Films*, 383 (2001) 154-160. [https://doi.org/10.1016/s0040-6090\(00\)01594-7](https://doi.org/10.1016/s0040-6090(00)01594-7)
- [55] W. Beyer, H. Wagner, The role of hydrogen in a-Si:H — results of evolution and annealing studies, *J. Non-Cryst. Solids*, 59-60 (1983) 161-168. [https://doi.org/10.1016/0022-3093\(83\)90547-1](https://doi.org/10.1016/0022-3093(83)90547-1)
- [56] W. Beyer, Hydrogen incorporation, stability, and release effects in thin film silicon, *Physica Status Solidi a-Applications and Materials Science*, 213 (2016) 1661-1674. <https://doi.org/10.1002/pssa.201532976>
- [57] Z.P. Wu, W.Y. Duan, A. Lambert, D.P. Qiu, M. Pomaska, Z.R. Yao, U. Rau, L.P. Zhang, Z.X. Liu, K.N. Ding, Low-resistivity p-type a-Si:H/AZO hole contact in high-efficiency silicon heterojunction solar cells, *Appl. Surf. Sci.*, 542 (2021) 7. <https://doi.org/10.1016/j.apsusc.2020.148749>
- [58] E. Gericke, J. Melskens, R. Wendt, M. Wollgarten, A. Hoell, K. Lips, Quantification of Nanoscale Density Fluctuations in Hydrogenated Amorphous Silicon, *Phys. Rev. Lett.*, 125 (2020) 185501. <https://doi.org/10.1103/PhysRevLett.125.185501>
- [59] N. Pham, Y. Djeridane, A. Abramov, A. Hadjadj, P. Roca i Cabarrocas, Role of Hydrogen in the Peeling of Hydrogenated Microcrystalline Silicon Films, *Mater. Sci. Eng., B*, 159-160 (2009)

- 27-30. <https://doi.org/10.1016/j.mseb.2008.11.021>
- [60] N. Pham, A. Hadjadj, P. Roca i Cabarrocas, O. Jbara, F. Kail, Interpretation of the hydrogen evolution during deposition of microcrystalline silicon by chemical transport, *Thin Solid Films*, 517 (2009) 6225-6229. <https://doi.org/10.1016/j.tsf.2009.02.072>
- [61] F. Kail, A. Hadjadj, P. Roca i Cabarrocas, Hydrogen diffusion and induced-crystallization in intrinsic and doped hydrogenated amorphous silicon films, *Thin Solid Films*, 487 (2005) 126-131. <https://doi.org/10.1016/j.tsf.2005.01.049>
- [62] A. Fontcuberta i Morral, P. Roca i Cabarrocas, Role of hydrogen diffusion on the growth of polymorphous and microcrystalline silicon thin films, *Eur. Phys. J. Appl. Phys.*, 35 (2006) 165-172.
- [63] B. Kalache, A.I. Kosarev, R. Vanderhaghen, P.R.i. Cabarrocas, Ion bombardment effects on microcrystalline silicon growth mechanisms and on the film properties, *J. Appl. Phys.*, 93 (2003) 1262-1273. <https://doi.org/10.1063/1.1524707>
- [64] H.P. Zhou, M. Xu, S. Xu, L.L. Liu, C.X. Liu, L.C. Kwek, L.X. Xu, Hydrogen-plasma-induced Rapid, Low-Temperature Crystallization of mum-thick a-Si:H Films, *Scientific Reports*, 6 (2016) 32716. <https://doi.org/10.1038/srep32716>
- [65] H. Shirai, J. Hanna, I. Shimizu, Role of Atomic-Hydrogen during Growth of Hydrogenated Amorphous-Silicon in the Chemical Annealing, *Jpn J Appl Phys* 2, 30 (1991) L679-L682. <https://doi.org/10.1143/jjap.30.L679>

Graphical Abstract

